RSC Advances

PAPER

View Article Online
View Journal | View Issue

Cite this: *RSC Adv.*, 2020, **10**, 1639

The polydopamine-enhanced superadhesion and fracture strength of honeycomb polyurethane porous membranes†

Mingshan Xue,‡[a] Dan Zhou,‡[a] Yuwei Ji,[a] Yu Xie,*[ab] Changquan Li[c] and Jinsheng Zhao*[b]

The superhydrophobic properties of biological surfaces in nature have attracted extensive attention in scientific and industrial circles. Relative to the rolling superhydrophobic state of lotus leaves, the adhesive superhydrophobic state of geckos and *Parthenocissus tricuspidata* is also significant in many fields. In this work, polydopamine (PDA) with its excellent biological compatibility and strong adhesion was selected as a substance to simulate the secretion of the suckers of *P. tricuspidata* and it was precipitated at the surface of honeycomb polyurethane porous membranes (PUPM). The results demonstrated that the honeycomb PUPM, as prepared, displayed special super-adhesion properties similar to those of geckos and *P. tricuspidata*. PDA formed *via* self-polymerization in aqueous solution was equivalent to a double-sided adhesive, acquiring a micro–nano structure of PDA and PUPM and displaying increased surface hydrophobicity and improved adhesion properties. Even when the surface precipitation of PDA and modification with *n*-dodecyl mercaptan made the contact angle increase to more than 160°, the surface adhesion to water was rather strong and remained stable. The addition of the PDA adhesive can effectively change the microporous structure of PUPM, enhancing the viscosity, and facilitating an enhancement in the fracture strength.

Received 28th September 2019
Accepted 28th November 2019

DOI: 10.1039/c9ra07887h

rsc.li/rsc-advances

1. Introduction

Bionics is the product of human learning from nature, and has made great contributions to human development and progress. With the continuous development of bionics, there have been many bionic studies on animal and plant parts displaying hydrophobic properties, such as lotus leaves, duck feathers and butterfly wings, *etc*[1–3]. In particular, the superhydrophobic properties of biological surfaces in nature have attracted extensive attention from scientific and industrial circles.[3,4] However, more research on the wettability of animal and plant surfaces displaying strong adhesion needs to be done. Scientists have studied the surfaces of lotus leaves and rose petals and other plants by using scanning electron microscopy and contact angle meters.[5] The wettability has been shown from many experiments to be mainly determined by the surface microscopic geometric structure and surface chemical composition.[6,7]

Early studies on adhesive materials mainly focused on animal and plant biology and physiology.[8,9] The representative subjects of such studies have been the gecko and *Parthenocissus tricuspidata*. Investigations of the surface structure of *P. tricuspidata* and analysis of the development of the suckers have resulted in improved understandings of tendril development, mucus secretion, morphological structure and other aspects.[10,11] Targeted scientific exploration has been carried out by combining materials science, physical chemistry, micro design and measurements, nanobionics, and other disciplines. For example, Endress *et al.*[12] studied the morphological and structural characteristics and adhesive properties of sucker organs of the highly adhesive *P. tricuspidata*. The nanoscale particles formed between the surface and the secretion of the suckers were observed using atomic force microscopy.[13] The positions of these nanoparticles and their functional effects on the adhesion of the sucker were analyzed.[14] These results indicated the presence of as many as 19 components in the viscous fluid, and that these nanoparticles play a significant and direct role in the adhesion process. Steinbrecher *et al.*[15] used cytochemical staining to find that the fully mature suckers have a special porous shape. Secreted mucus has been demonstrated to occupy the porous cells of the epidermis and to extend into the depressions, leading to an essentially perfect occlusive

[a]School of Materials Science and Engineering, Nanchang Hangkong University, Nanchang 330063, People's Republic of China. E-mail: xieyu_121@163.com; Fax: +86 791 83953373; Tel: +86 791 83953408

[b]Department of Chemistry and Chemical Engineering, Liaocheng University, Liaocheng, 252059, People's Republic of China. E-mail: j.s.zhao@163.com

[c]School of Materials and Engineering, Jiangsu University of Technology, Changzhou, Jiangsu 213001, People's Republic of China

† Electronic supplementary information (ESI) available. See DOI: 10.1039/c9ra07887h

‡ These authors contributed equally to this work.

contact between the suckers and the base surface, and hence resulting in superadhesion.[16]

Utilizing the strong adhesion of such adhesive materials in medical applications involving antifouling is highly promising.[17] Furthermore, these materials have good biocompatibility and can also be used in the field of biomedical materials such as artificial blood vessels.[18] Scientists have simulated the micro–nano structure of the mature surface of the *P. tricuspidata*. Some studies have shown a nearly complete lack of adsorption of platelets onto the surfaces of superhydrophobic polyurethane (PU) porous films,[19] while platelets have been observed to be adsorbed onto the hydrophobic surfaces of smooth PU porous films. The superhydrophobic adhesive materials exhibit better biocompatibility than do common materials, and this better biocompatibility opens up a new research direction for the development of biomedical materials.[20–23]

Adhesive materials in modern medicine, food and industry also have great potential development value, and more attention should be paid to the comprehensive exploitation and utilization of such materials, and to strengthen their biological medicinal value and industrial applications.[24] In the work described in this paper, polydopamine (PDA) with its excellent biological compatibility and strong adhesion was selected as a substance to simulate the secretion of the suckers of *P. tricuspidata* in order to find a kind of material displaying strong adhesion. Specifically, PDA-enhanced superadhesion and fracture strength of honeycomb polyurethane porous membranes (PUPM) were focused on. The prepared honeycomb PUPM displayed special superadhesion properties, similar to those of the geckos and *P. tricuspidata*. The growth of PDA on PUPM was first investigated, followed by the effect of PDA on the fracture strength of PUPM, and finally the effect of PDA on the surface wettability of PUPM.

2. Materials and methods

2.1 Principle of preparing PUPM using microphase separation

In a solution, a dynamic equilibrium between solubility and crystallization can be reached. At this point, the solid polymer would continuously dissolve into the polymer solution, and the polymer from the saturated polymer would solution would keep on crystallizing, thus resulting in a dynamically variable crystal configuration. According to the principle of minimum surface free energy, the surface free energy is inversely proportional to crystal volume. So near thermodynamic equilibrium, the volume of the crystal would always tend to become large during a slow crystallization.

The principle behind the growth of PUPM in the current work was developed based on the use of a viscous solution mixed with tetrahydrofuran and PU as the basic reactants.[25,26] In a homemade box, a dynamic equilibrium was achieved between the entrance of water molecules and the volatilization of tetrahydrofuran. While water molecules continuously entered the solution on the surface of the sample, tetrahydrofuran molecules also continuously volatilized into the air, and then PU solidified on the substrate surface to form chain segments. The PU on the surface of the substrate began to cure, and form so-called thick and thin phases of microscopic size. The thin phase gradually formed the pores. As the curing time was increased, the thick phase became thicker and the thin phase became thinner, finally forming regular and ordered honeycomb PUPM.

The epidermis of mature *P. tricuspidata* secretes a kind of hydrochloric polysaccharide having a very considerable effect on the adhesion. In the current work, dopamine hydrochloride instead of polysaccharide was deposited on the surface of the honeycomb PUPM. Specifically, the honeycomb PUPM were put into a freshly prepared dopamine solution (pH = 8.5), and then taken out of the solution after a specified period of time. In this way, a tightly adhered cross-linking dopaminergic composite layer formed on the surface of the honeycomb PUPM.

2.2 Characterizations of the PUPM

The surface microstructures of the PUPM were characterized using field emission scanning electron microscopy (FESEM, FEI, USA) with an accelerating voltage of 10 kV. The main chemical constituents of the PUPM were identified by using FESEM-energy dispersive spectroscopy (EDS). The contact angle (CA) and rolling angle (RA) of each sample were investigated by using a contact angle meter (DSA20, Kruss, Germany) to analyze the wettability of the sample surface. The droplet volume was 4 μL and the shown contact angle of each sample was the average value of contact angles measured in five different positions. The tensile performances of the PUPM were measured by using an electronic universal testing machine (UTM4203, Kason, China). The stretching distance applied to the samples with dimensions of $10 \times 100 \times 2$ mm^3 was 100 mm, and the stretching speed applied was 100 mm min^{-1}. The average value was taken from five samples in each group.

3. Results

3.1 Growth of PDA on the PUPM

The PUPM were prepared by carrying out microphase separation, as shown in the SEM images of Fig. 1(a) and (b). A PU solution with a mass fraction of 2% was prepared, and the relative humidity in the chamber of the in-house-made reaction device was controlled to be 100%. After the surface was completely cured and the membranes were dried in an oven for 1 h, a clear honeycomb porous structure was formed and the average size of these pores was about 5 μm.

The suckers of mature *P. tricuspidata* have a honeycomb porous structure with a viscous fluid. PDA was selected as the substance secreted by the bionic *P. tricuspidata* because of its excellent biological compatibility and especially strong adhesion, characteristics also displayed by the viscous fluid.[27] PDA formed by self-polymerization in aqueous solution displayed natural adhesion, equivalent to a double-sided adhesive. PDA layers were prepared at the surfaces of the PUPM by immersing PDA into alkaline dopamine buffer solutions for a specified period of time. Fig. 1(c) and (d) show the SEM images of the

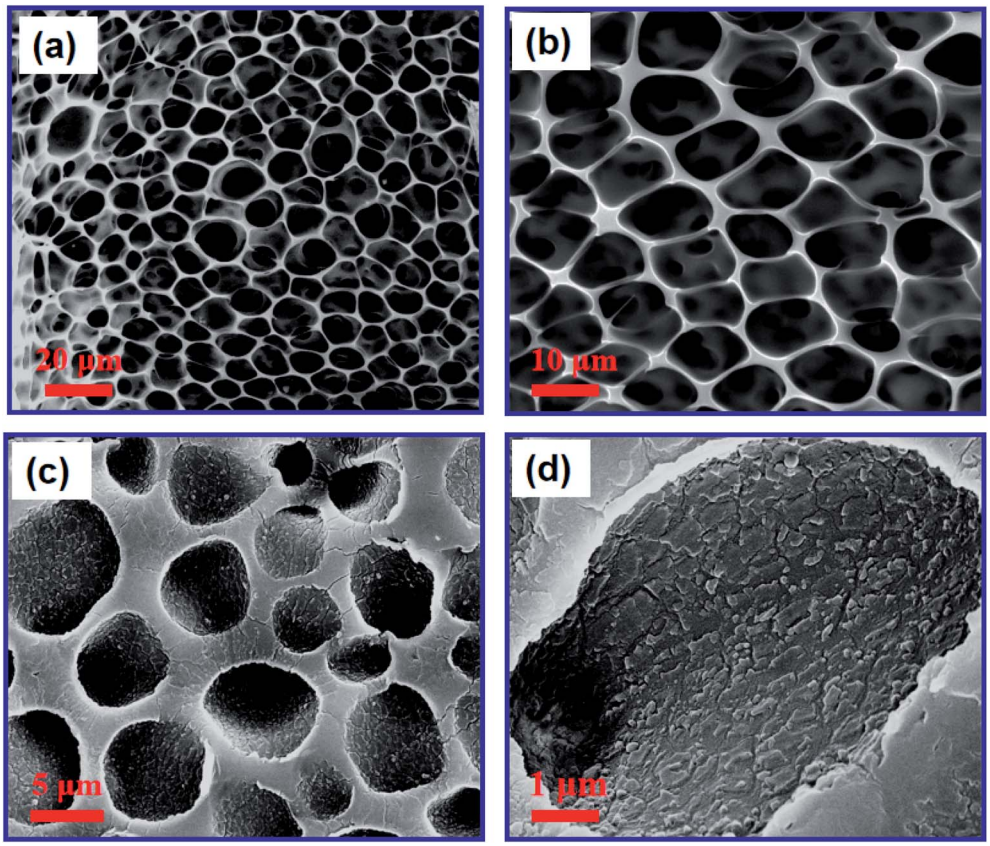

Fig. 1 SEM images of the prepared PUPM. (a) Regular-magnification and (b) high-magnification images of the PUPM formed in PU solution with a mass fraction of 2% and relative humidity of 100%. High-magnification images of (c) PUPM after the precipitation of PDA and (d) an inner wall of a single pore of PUPM after being coated with PDA.

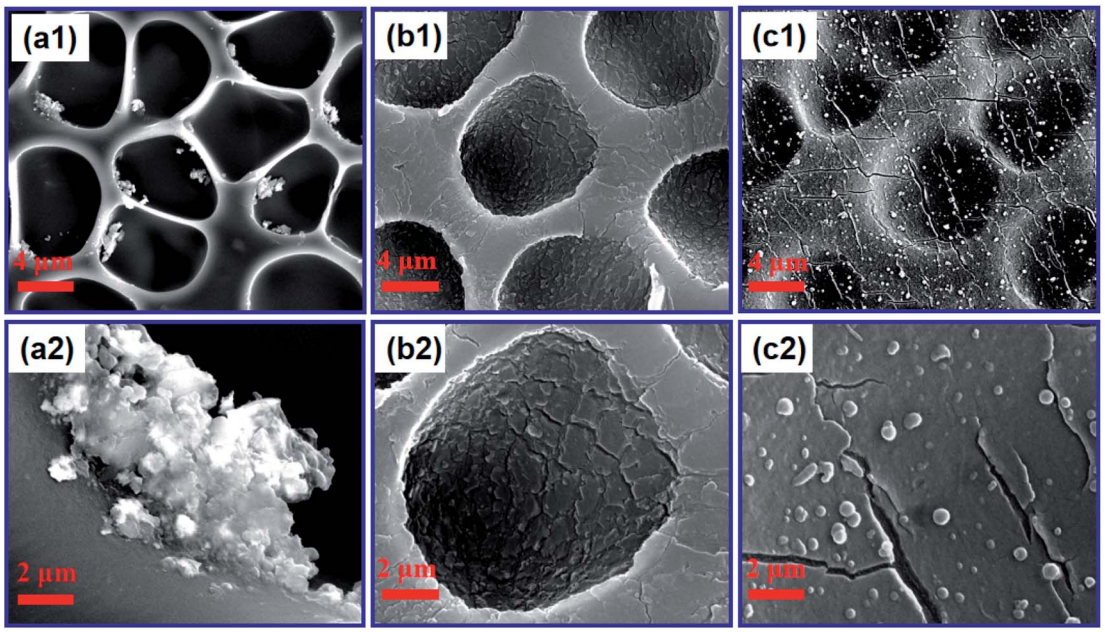

Fig. 2 SEM images of PUPM after precipitating PDA from solutions with different concentrations of dopamine hydrochloride: (a1 and a2) 1 g L^{-1}, (b1 and b2) 2 g L^{-1}, and (c1 and c2) 3 g L. (a2–c2) High-magnification images of (a1–c1).

PUPM after being coated with PDA. Here the pH of the film in the buffer solution was controlled to be 8.5, and the reaction time was 24 h. Dopamine hydrochloride was observed to form mastoid-shaped structures with dimensions of about 200 nm on the porous wall surface of the PUPM. The cross-sectional SEM images of PUPM before and after being functionalized with PDA are shown in Fig. S1.† In these images, there was no obvious boundary seen at the interface besides the increase of the thickness of the membranes, indicating that the PDA formed by self-polymerization in aqueous solution was a good double-sided adhesive.

Fig. 2 shows the effect of the concentration of dopamine hydrochloride on the surface morphology of the PUPM. Accumulations of granular mastoid-shaped structures grew on the surfaces of the original cellular structure and in the pore walls. When the concentration of dopamine hydrochloride was 1 g L^{-1}, the honeycomb porous structure of PUPM was clearly visible. As the concentration was increased, an accumulation of dopamine gradually formed on the surfaces and inner walls of the pores, and the honeycomb pores became micropits. For example, when the concentration of dopamine hydrochloride was increased to 2 g L^{-1}, the porous surface transformed into solid pores and lost the original permeability, although the distribution of the pores remained uniform. When the concentration was increased to 3 g L^{-1}, these micropits were gradually filled up and made even. Owing to the high concentration of dopamine, the excessive free –OH in the solution polymerized with –C═O of PU *via* a condensation reaction, which altered the surface composition of the PUPM and changed the morphology of the membranes. As shown in Fig. 3, polymerization of the dissolved dopamine with the PUPM endowed the film surface with active functional groups. When the dopamine molecules came into contact with the polar water molecules, functional groups (hydroxyl, carbonyl or imino groups) at the surface of the PUPM formed polar interactions with the water molecules, so that the benzene rings and carbon chains in the membranes were more closely bound, and in this way achieved a better adhesive effect.[28]

Fig. 4 shows infrared spectra, acquired using a using Fourier transform infrared spectrometer, of the PUPM before and after their surfaces were modified with dopamine hydrochloride. The bands observed at 1732 cm^{-1}, 1631 cm^{-1}, 1258 cm^{-1} and 1170 cm^{-1} were attributed to ester C═O, amide C═O, ester C–O and ether bond C–O vibrations,[29] respectively. These bands weakened after application of the dopamine modification. In addition, bands observed at 3401 cm^{-1} and 2934 cm^{-1} and due to –NH– and –CH– stretch bonds, respectively, disappeared after the modification. This disappearance was attributed to the

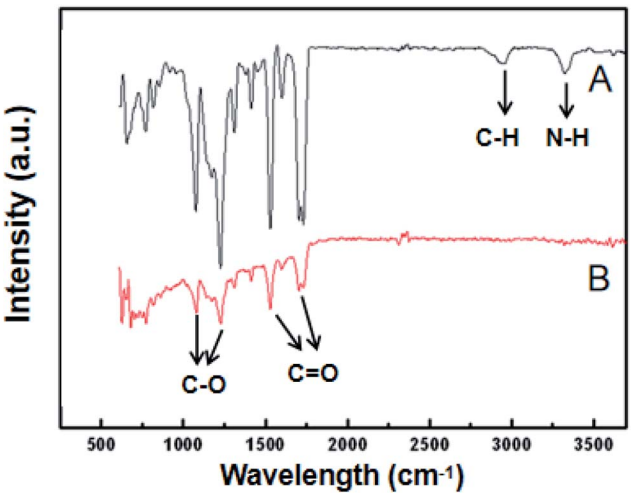

Fig. 4 Infrared spectra of PU porous membranes (A) before and (B) after being modified with PDA.

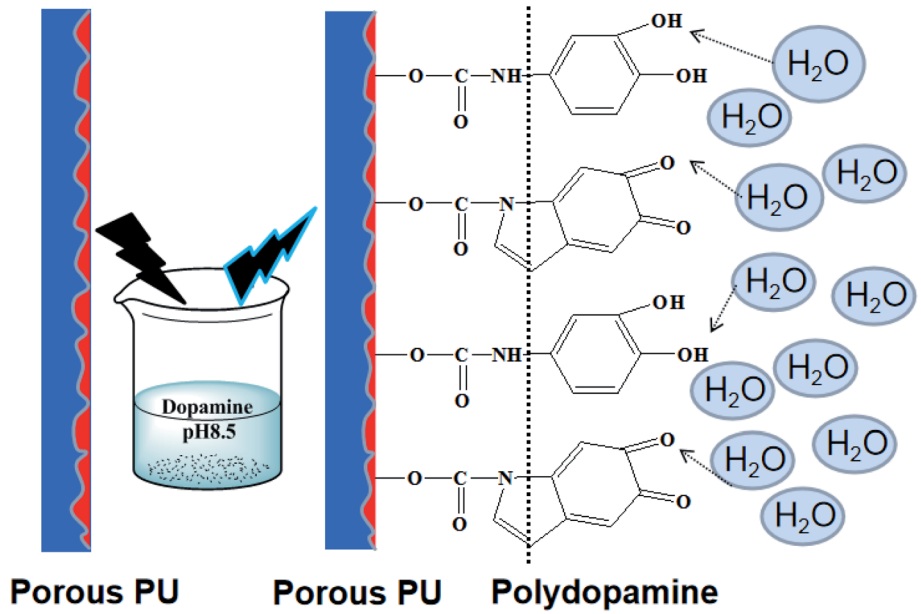

Fig. 3 The mechanism of the bonding of the honeycomb PUPM with PDA at the interface.

polymerization of dopamine, *via* its benzene ring and –OH and $–NH_2$ bonds, with the characteristic groups in the PU membranes.[30]

The X-ray diffraction patterns of the unmodified and PDA-modified PUPM (Fig. S2†) each showed a main peak at a two-theta angle of 21.74°, corresponding to lattice constants of $a = 4.787$ nm, $c = 12.015$ nm for the PU crystal.[31] These diffractions patterns were similar except that the peak of the modified sample was weaker, results together indicating a poorer crystallinity but otherwise similar overall structure of this sample.

3.2 Effect of PDA on the fracture strength of PUPM

The mechanical properties of honeycomb PUPM are very important for their practical applications. Fig. 5 shows the fracture strengths of the unmodified and PDA-modified PUPM. In the unmodified case, the fracture strength of honeycomb PUPM increased with increasing mass fraction of PU in the solution used to prepare the PUPM. As shown in the insets of Fig. 5, as-prepared PUPM at higher concentrations showed more but smaller pores, with thicker walls between these pores. That is, in these cases, regular honeycomb PUPM were not easily achieved, attributed to the high concentration not having been conducive to the volatilization of the tetrahydrofuran solvent and hence hindering the rearrangement and movement of PU. And the regular honeycomb PUPM formed under low concentration showed low fracture strength, on account of the large pores and thin pore walls. In sharp contrast to the case of the pure PUPM, the fracture strengths of the samples of PDA-modified PUPM were greater. The highest fracture strength value of the PU porous membranes, at 15.1 MPa, was achieved when using a polydopamine mass fraction of 8% and PDA concentration of 3 g L^{-1}. On the one hand, as the concentration of PU in the solution was increased, the dispersion of the thick and thin phases on the surfaces of the membranes was more rapid in the process of forming the PUPM, and the microporous structure was more dense and solid, leading to the increase of the fracture strength. On the other hand, the addition of the adhesive PDA changed the microporous structure of the PUPM (Fig. 2), namely partly filling up the pores and making the pore walls thicker. Furthermore, the fracture strength testing process not only showed an increase in fracture strength resulting from the PDA modification of the PUPM, but also did not yield any obvious cracks according to inspection of cross-sectional SEM images (Fig. S3†), suggesting a positive role played by the PDA adhesive in enhancing the mechanical properties of the PUPM.

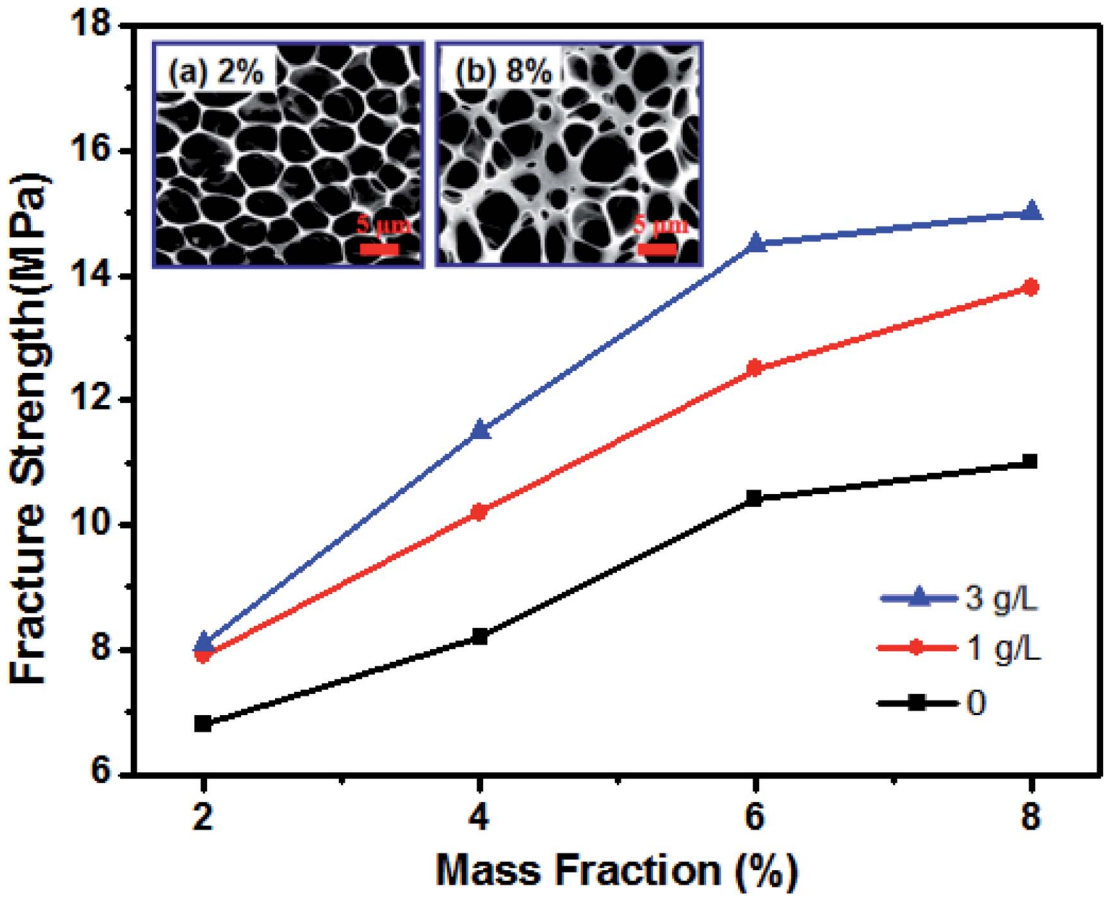

Fig. 5 Fracture strengths of the unmodified (black) and PDA-modified PUPM (red and blue), each as a function of the mass fraction of PU in the solution used to prepare the PUPM. The two tested samples of PDA-modified PUPM were prepared using, respectively, 1 g L^{-1} and 3 g L^{-1} dopamine hydrochloride. The insets show SEM images of PUPM formed using PU mass fractions of (a) 2% and (b) 8%.

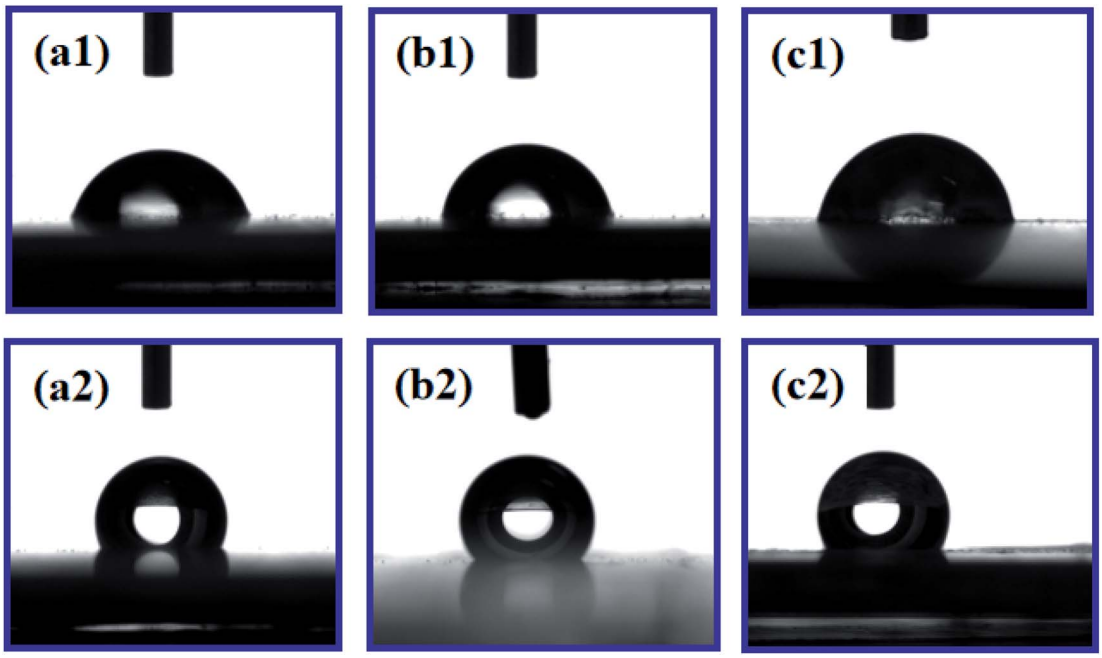

Fig. 6 Photographs showing water droplets on the surfaces of PUPM (a1–c1) before and (a2–c2) after being coated with PDA made using (a2) 1 g L^{-1}, (b2) 2 g L^{-1}, and (c2) 3 g L^{-1} dopamine hydrochloride. CAs of the droplets were derived from these images.

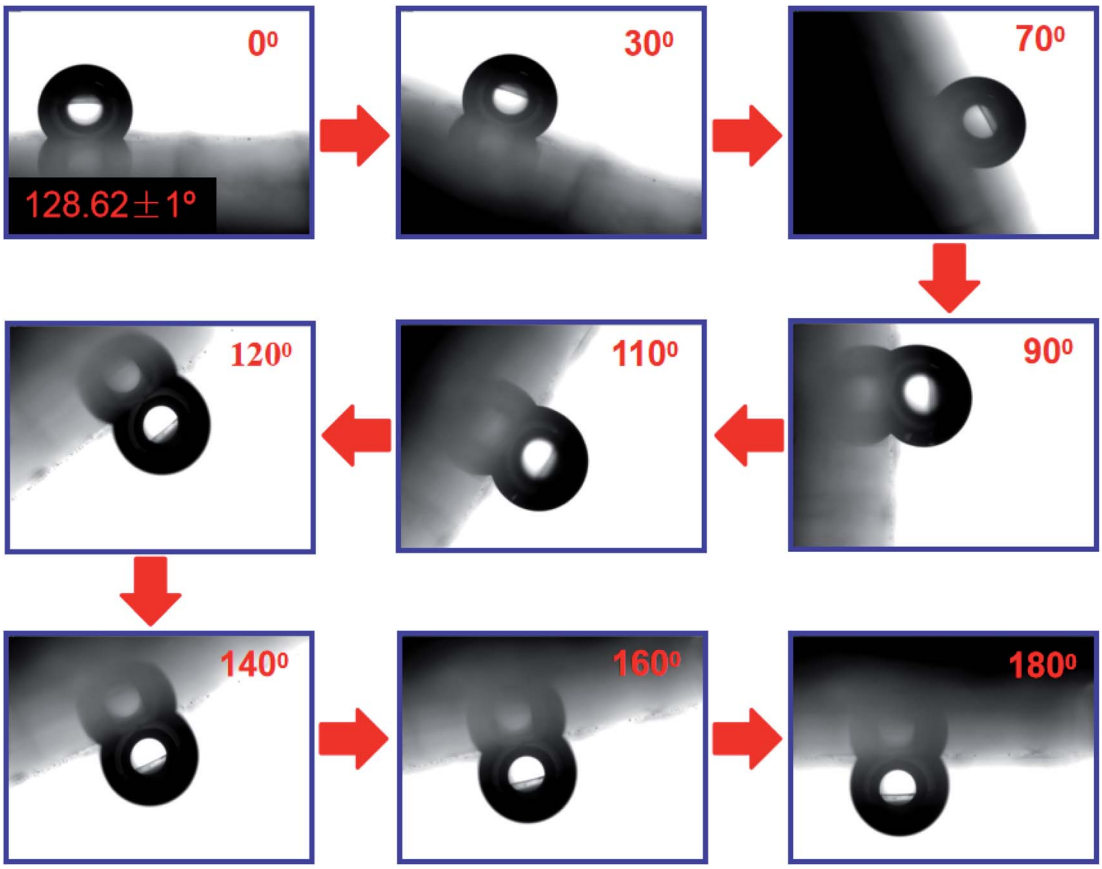

Fig. 7 Photographs of a water droplet with a CA of 128.62° on the surface of a sample of PDA-modified PUPM that was rotated from right-side up to upside down.

3.3 Effect of PDA on surface wettability of PUPM

The addition of PDA changed the fracture strength and surface roughness of PUPM. Apart from chemical composition, surface roughness is another important parameter that affects the surface wettability of a material. Fig. 6 shows photographs of water droplets on the surfaces of PUPM before and after their having been coated with PDA made using various concentrations of dopamine hydrochloride, and CAs of the droplets were derived from these images. When the concentration of dopamine used was 2 g L^{-1}, the contact angle was 128.62°, higher than the 120.19° value when the concentration was 1 g L^{-1}. This result demonstrated that the viscous dopamine precipitated into pores and changed the surface roughness levels of the PU pores, which increased the longitudinal contact area with water and caused an increase in the CA. According to wetting theory,[32–34] there are two basic models (the Wenzel model and the Cassie–Baxter model) used to explain the hydrophobicity of solid surfaces. The Wenzel model is based on water droplets infiltrating into the pores at the topmost surface (just as in the present case), while the Cassie–Baxter model is based on the water droplets being suspended on the top of the surface of the micro-convex body. Our SEM images of the PDA-modified PUPM (Fig. 2) indicated the formation of a bumpy and mastoid-shaped structure instead of a flat film inside and outside of the hole walls, leading to an increase of the surface roughness and corresponding CA according to the Wenzel model.

Fig. 7 displays dynamic images of the RA of water droplets on the surface of PDA-modified PUPM. After the sample was

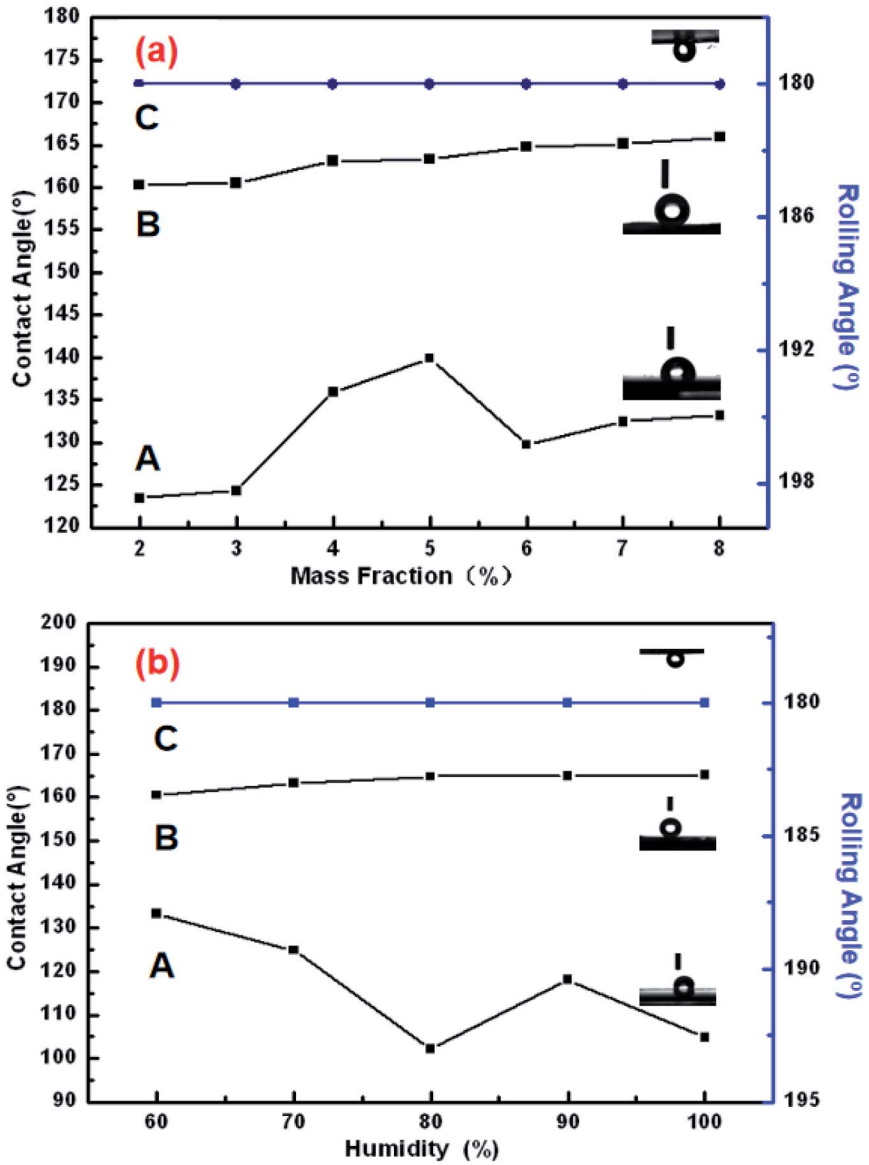

Fig. 8 CAs of water droplets on the surfaces of PDA-precipitated PUPM grown in (a) solutions of different PU concentrations and (b) different relative humidity levels (A) before and (B) after being modified with *n*-dodecyl mercaptan. The blue lines (C) give the corresponding RA after the modification with *n*-dodecyl mercaptan.

rotated by 180°, the water droplets remained stable on the surface. This strong adhesion for water displayed by the PDA-coated honeycomb structures was attributed to their surface porous morphology and high surface free energy. Here, PDA was concluded to mainly play two roles. On the one hand, its equivalence to a double-sided adhesive, as a result of the inherently high adhesion of the PDA, resulted in the increased adhesion of water to its surface. On the other hand, the average diameter of the PU pores was 2–5 μm, while the average diameter of the mastoid-shaped particles of PDA on PUPM was about 50–400 nm. Such a micro–nano structure consisting of PDA and PUPM increased the surface roughness, improving the surface hydrophobicity and adhesive properties. It has been noticed that different negative pressures produced by different volumes of sealed air could be a crucial factor for different adhesions [35,36]. So the adhesive forces of the as-prepared PUPM for water might be effectively controlled by varying the amount of PDA on the surfaces of PUPM, which effectively adjusted the negative pressures that were produced as a result of changing the pores.

Note that when the sample surface was rotated by 180°, the water droplets deformed, due to gravity, and showed a tendency to roll downward, but did not roll out, showing an obvious contact angle hysteresis. Even when shaking the sample, the water droplets still adhered to the sample surface firmly, showing that the strong adhesion of the sample surface for the water droplets was sufficient to balance the weight of the water droplets themselves. Fig. 8 shows the CAs and RAs of PDA-PUPM membranes prepared using different concentrations and humidity levels before and after being subjected to surface modification with *n*-dodecyl mercaptan with low surface energy. After the surface modification, the CA was more than 160°, but different from that of the rolling superhydrophobic state of lotus leaves. Instead, the water droplets always adhered to the surface when the sample was rotated by 180°, indicating the adhesive superhydrophobic state.

Inspection of the SEM images of the various samples of dopamine-modified PUPM showed that as the dopamine concentration in the solution was increased, the pores became denser and the surface adhesion became stronger. These results combined with examinations of the morphology of PUPM prepared under different humidity levels indicated that the pores did not form easily at low humidity, and that the as-prepared pores were disordered, so the surface roughness was low. However, the CA was more than 160° and the surface adhesion to water was considerable and rather stable after surface precipitation of PDA and modification with *n*-dodecyl mercaptan. These results showed that the addition of PDA can enhance the adhesion of water to the surface of PUPM.

4. Conclusions

PDA samples at various concentrations were precipitated at the surface of honeycomb PUPM to simulate the secretion of the suckers of *P. tricuspidata*. The honeycomb PUPM were found to display especially strong adhesion, similar to those of geckos and *P. tricuspidata*. Moreover, PDA formed by self-polymerization in aqueous solution was shown to be equivalent to a double-sided adhesive, forming a micro–nano structure consisting of PDA and PUPM and dramatically increasing the surface hydrophobicity and adhesion. Including the surface precipitation of PDA and modification with *n*-dodecyl resulted in an increase of the CA to more than 160°, and led to the rather strong and stable adhesion of water onto the surface of PUPM. The addition of the PDA was found to change the microporous structure of PUPM, increasing the viscosity, and contributing to an enhancement in the tensile strength. These results are expected to benefit the exploration of new functional materials with especially strong adhesion at levels similar to those displayed by geckos and *P. tricuspidata*.

Conflicts of interest

There are no conflicts to declare.

Acknowledgements

This work was financially supported by the National Natural Science Foundation of China (No. 51662032, 21667019, 11864024, 51703091, 21965023), the Key Project of the Natural Science Foundation of Jiangxi Province (No. 20171ACB20016, 20171BAB216005), the Jiangxi Province Major Academic and Technical Leaders Cultivating Object Program (No. 20172BCB22014), the Science and Technology Department of Jiangxi Province (No. 20181BCB18003 and 20181ACG70025, 20181BAB216012), the Key Laboratory of Photochemical Conversion and Optoelectronic Materials, TIPC, CSA (No. PCOM201906), the Key Project of Science and Technology Research of the Jiangxi Provincial Department of Education (No. DA201602063, DA201802151), Fujian Key Laboratory of Measurement and Control System for of Shore Environment (No. S1-KF1703) and the Qing Lan Project of Jiangsu Province.

References

1 R. A. Laura, P. Alessandro, R. P. Lorena, S. Edoardo, N. Kamolchanok and B. Giuseppe, *Biomaterials*, 2019, **192**, 26–50.
2 W. Barthlott, M. Mail and C. Neinhuis, *Philos. Trans. R. Soc., A*, 2016, **374**, 2073.
3 X. Gou and Z. Guo, *J. Bionic Eng.*, 2018, **15**, 851–858.
4 Y. Si, Z. Dong and L. Jiang, *ACS Cent. Sci.*, 2018, **4**, 1102–1112.
5 S. Wang and L. Jiang, *Adv. Mater.*, 2010, **19**, 3423–3424.
6 L. Feng, S. Li, H. Li, J. Zhai, Y. Song, L. Jiang and D. Zhu, *Angew. Chem., Int. Ed.*, 2002, **41**, 1221–1223.
7 J. Wu, H. J. Bai, X. B. Zhang, J. J. Xu and H. Y. Chen, *Langmuir*, 2010, **26**, 1191–1198.
8 Y. Zheng, X. Gao and L. Jiang, *Soft Matter*, 2007, **3**, 178–182.
9 J. Yong, Q. Yang, F. Chen, D. Zhang, G. Du, H. Bian, J. Si and X. Hou, *RSC Adv.*, 2014, **4**, 8138.
10 M. Cáceres, R. Hidalgo, A. Sanz, J. Martínez, P. Riera and P. C. Smith, *J. Periodontol.*, 2008, **79**, 714–720.
11 X. Yang and W. Deng, *Chin. Sci. Bull.*, 2014, **59**, 113–124.

12 A. G. Endress and W. W. Thomson, *Can. J. Bot.*, 1977, **55**, 918–924.
13 A. J. Bowling and K. C. Vaughn, *Protoplasma*, 2008, **232**, 153–163.
14 T. Steinbrecher, E. Danninger, D. Harder, T. Speck, O. Kraft and R. Schwaiger, *Acta Biomater.*, 2010, **6**, 1497–1504.
15 T. Steinbrecher, G. Beuchle, B. Melzer, T. Speck, O. Kraft and R. Schwaiger, *Int. J. Plant Sci.*, 2011, **172**, 1120–1129.
16 H. K. Yasuda, Q. S. Yu, C. M. Reddy, C. E. Moffitt and D. M. Wieliczka, *J. Appl. Polym. Sci.*, 2002, **85**, 15–20.
17 J. H. Roh, J. H. Lee and T. H. Yoon, *J. Adhes. Sci. Technol.*, 2002, **16**, 1529–1543.
18 A. Synytska, E. Svetushkina, N. Puretskiy, G. Stoychev, S. Berger, L. Ionov, C. Bellmann, K. J. Eichhorna and M. Stamma, *Soft Matter*, 2010, **6**, 5907–5914.
19 T. Sun, H. Tan, D. Han, Q. Fu and L. Jiang, *Small*, 2005, **1**, 959–963.
20 Y. Lai, X. Gao, H. Zhuang, J. Huang, C. Lin and L. Jiang, *Adv. Mater.*, 2009, **21**, 3799–3803.
21 C. B. Ge, W. T. Zhai and C. B. Park, *Polymers*, 2019, **11**, 847.
22 A. P. Isfahani, M. Sadeghi, K. Wakimoto, B. B. Shrestha, R. Bagheri, E. Sivaniah and B. Ghalei, *ACS Appl. Mater. Interfaces*, 2018, **10**, 17366–17374.
23 L. Zhu, X. Zhou, Y. h. Liu and Q. Fu, *ACS Appl. Mater. Interfaces*, 2019, **11**, 12968–12977.
24 K. Tan and S. K. Obendorf, *J. Membr. Sci.*, 2006, **274**, 150–158.
25 M. Kiremitci, M. Pulat, C. Senvar, A. I. Serbetci and E. Piskin, *Clin. Mater.*, 1990, **6**, 227–237.
26 M. Pulat and C. Senvar, *Polym. Test.*, 1995, **14**, 115–120.
27 X. Zhang, S. Wang, L. Xu, L. Feng, Y. Ji, L. Tao, S. Li and Y. Wei, *Nanoscale*, 2012, **4**, 5581.
28 G. Han, S. Zhang, X. Li, N. Widjojo and T.-S. Chung, *Chem. Eng. Sci.*, 2012, **80**, 219–231.
29 K. Tan and S. K. Obendorf, *J. Membr. Sci.*, 2007, **289**, 199–209.
30 G. Z. Ke, H. F. Xie, R. P. Ruan and W. D. Yu, *Energy Convers. Manage.*, 2010, **51**, 2294–2298.
31 V. Melnig, M. O. Apostu, V. Tura and C. Ciobanu, *J. Membr. Sci.*, 2005, **267**, 58–67.
32 D. Murakami, H. Jinnai and A. Takahara, *Langmuir*, 2014, **30**, 2061–2067.
33 M. Xue, Y. Ji, J. Ou, F. Wang, C. Li, S. Lei and W. Li, *AIP Adv.*, 2019, **9**, 075309.
34 A. M. Peters, C. Pirat, M. Sbragaglia, B. M. Borkent, M. Wessling, D. Lohse and R. G. H. Lammertink, *Eur. Phys. J. E*, 2009, **29**, 391–397.
35 L. Heng, X. Meng, B. Wang and L. Jiang, *Langmuir*, 2013, **29**, 9491–9498.
36 K. Han, L. Heng and L. Jiang, *ACS Nano*, 2016, **10**, 11087–11095.